

A novel alternate secretory pathway for the export of *Plasmodium* proteins into the host erythrocyte

(malaria/apicomplexa/brefeldin A/protein transport)

MARK F. WISER*[†], H. NORBERT LANNERS[‡], RICHARD A. BAFFORD*, AND JENNY M. FAVALORO[§]

*Department of Tropical Medicine, Tulane University School of Public Health, New Orleans, LA 70112; [‡]Tulane Regional Primate Research Center, Covington, LA 70433; and [§]Department of Medicine, Royal Melbourne Hospital, Parkville, Victoria 3050, Australia

Communicated by William Trager, Rockefeller University, New York, NY, June 23, 1997 (received for review March 28, 1997)

ABSTRACT The malarial parasite dramatically alters its host cell by exporting and targeting proteins to specific locations within the erythrocyte. Little is known about the mechanisms by which the parasite is able to carry out this extraparasite transport. The fungal metabolite brefeldin A (BFA) has been used to study the secretory pathway in eukaryotes. BFA treatment of infected erythrocytes inhibits protein export and results in the accumulation of exported *Plasmodium* proteins into a compartment that is at the parasite periphery. Parasite proteins that are normally localized to the erythrocyte membrane, to nonmembrane bound inclusions in the erythrocyte cytoplasm, or to the parasitophorous vacuolar membrane accumulate in this BFA-induced compartment. A single BFA-induced compartment is detected per parasite and the various exported proteins colocalize to this compartment regardless of their final destinations. Parasite membrane proteins do not accumulate in this novel compartment, but accumulate in the endoplasmic reticulum (ER), suggesting that the parasite has two secretory pathways. This alternate secretory pathway is established immediately after merozoite invasion and at least some dense granule proteins also use the alternate pathway. The BFA-induced compartment exhibits properties that are similar to the ER, but it is clearly distinct from the ER. We propose to call this new organelle the secondary ER of apicomplexa. This ER-like organelle is an early, if not the first, step in the export of *Plasmodium* proteins into the host erythrocyte.

The malarial parasite invades and infects an erythrocyte during one stage of its life cycle. During this intraerythrocytic stage, the parasite extensively modifies the cytoplasm and the plasma membrane of the host erythrocyte. These modifications include the appearance of membranous clefts and vesicles, as well as nonmembrane bound aggregates of parasite proteins within the host cell cytoplasm. Ultrastructural changes of the host erythrocyte membrane include the appearance of electron dense knobs and/or the formation of caveola-vesicle complexes on the surface of some *Plasmodium*-infected erythrocytes (1). Presumably such alterations are important for the survival of the parasite. Little is known about how the parasite carries out these modifications of the host erythrocyte. The problem is more complex than the parasite simply secreting proteins into the host erythrocyte. The membrane bound clefts and the nonmembrane bound aggregates are distinct compartments within the infected erythrocyte (2, 3) and parasite proteins are specifically targeted to these various intraerythrocytic compartments including the host membrane. This extraparasite transport process cannot rely upon the intracellular transport machinery of the host cell

since the mature erythrocyte completely lacks internal membranes and organelles. Thus, the parasite has the ability to transport and target proteins to compartments beyond its own plasma membrane.

Eukaryotic cells efficiently target proteins to different intracellular compartments. This intracellular transport and sorting is carried out by the endoplasmic reticulum (ER) and Golgi apparatus via vesicles (4). The malaria parasite's ER and Golgi apparatus are not well characterized morphologically and have only been described as loosely associated vesicles (5, 6). In addition, some of the proteins involved in the eukaryotic secretory pathway have been identified in *Plasmodium falciparum* (7–10). Brefeldin A (BFA) is a fungal metabolite that inhibits protein secretion and has been used to investigate the secretory pathway (11). BFA also inhibits the export of parasite proteins destined for various compartments within the infected erythrocyte (12–15), suggesting that the parasite's secretory pathway is involved in the export of proteins into the host erythrocyte.

To learn more about extraparasite transport in *Plasmodium*, we examined the fate of exported proteins after BFA treatment. BFA treatment results in the accumulation of exported *Plasmodium* proteins into a novel compartment at the parasite periphery. This BFA-induced compartment exhibits some similarities to the ER, but it is distinct from the ER. These results demonstrate that the malarial parasite has two parallel secretory pathways: one is the normal intracellular secretory pathway and the other pathway specializes in the export and targeting of proteins into the host cell.

MATERIALS AND METHODS

Preparation of Infected Erythrocytes and Antibodies. *Plasmodium berghei* (K173 strain) and *Plasmodium chabaudi* (strain 54X) were obtained from H. Mühlfordt and R. Walter (Bernhard-Nocht-Institute, Hamburg, Germany), respectively, and maintained by serial passage in CD-1 outbred mice (Charles Rivers Laboratories). Mice were housed at the Tulane University Medical Center vivarium in accordance with applicable regulations. Parasitemia was monitored by Giemsa-stained thin blood smears obtained from tail snips. After axillary incision infected blood was collected with heparinized Pasteur pipettes and washed three times in RPMI 1640 medium. *P. chabaudi*-infected erythrocytes were collected between midnight and 0100 corresponding to the period of maximum schizont rupture and merozoite invasion. The infected erythrocytes were resuspended at a hematocrit of 5% in

Abbreviations: BFA, brefeldin A; ER, endoplasmic reticulum; MSP-1, merozoite surface protein-1; PVM, parasitophorous vacuolar membrane; sERA, secondary ER of the apicomplexa; TVM, tubovesicular membrane.

[†]To whom reprint requests should be addressed at: Department of Tropical Medicine, Tulane University Medical Center, 1501 Canal Street, New Orleans, LA 70112. e-mail: wiser@mailhost.tcs.tulane.edu.

The publication costs of this article were defrayed in part by page charge payment. This article must therefore be hereby marked "advertisement" in accordance with 18 U.S.C. §1734 solely to indicate this fact.

© 1997 by The National Academy of Sciences 0027-8424/97/949108-6\$2.00/0 PNAS is available online at <http://www.pnas.org>.

RPMI 1640 medium containing 10% fetal calf serum and incubated with BFA at 5–10 $\mu\text{g/ml}$. Controls were treated with 0.05–0.1% methanol. After incubation in a candle jar at 37°C (16), the infected erythrocytes were washed twice in Hanks' balanced salt solution and examined by immunofluorescence and immunoelectron microscopy as described below.

mAbs against *P. berghei* proteins, prepared from hyperimmune mice (17), include mAb F4.4 against merozoite surface protein 1 (MSP-1) (18) and mAb I2.6 and mAb W3.5 against 31-kDa and 13-kDa *P. berghei* proteins, respectively. Parasite proteins associated with the erythrocyte membrane have been purified and used to generate mAb 16.3 against a 65-kDa *P. berghei* protein, Pb(em)65, and mAb 13.5 against a 93-kDa *P. chabaudi* protein, Pc(em)93 (19). A monospecific polyclonal rabbit antiserum was raised against a 24-kDa *P. chabaudi* protein (Ag-3008) localized to the parasitophorous vacuolar membrane (PVM) (20). A rabbit antiserum raised against the last 11 amino acids of *P. falciparum* BiP (7) that also cross-reacts with *P. berghei* (21) was used as a marker for the ER.

Immunofluorescence and Preembedding Immunoelectron Microscopy. Infected erythrocytes were fixed with 0.025–0.05% glutaraldehyde for 10 min, treated with glycine, and washed in Hanks' balanced salt solution containing 1% BSA as described (22). The samples were then incubated with primary antibodies in the presence of 0.1% Triton X-100 for 1 hr at room temperature followed by three washes and incubation with fluorochrome-conjugated anti-mouse or anti-rabbit IgG (Sigma). After three more washes, the samples were examined for epifluorescence under UV illumination. Parasites were counterstained with ethidium bromide (10 $\mu\text{g/ml}$) as indicated. Samples for scanning confocal microscopy were mounted under a coverslip in 0.1 M Tris-HCl (pH 8.5) containing 25% glycerol, 10% polyvinyl alcohol, and 2.5% 1,4-diazabicyclo-[2.2.2]octane and examined with a Leica (model H20-004) confocal microscope.

The preembedding immunoelectron microscopy procedure was identical to the immunofluorescence assay except that ultrasmall (<1 nm) colloidal-gold-conjugated anti-mouse IgG (Electron Microscopy Sciences, Fort Washington, PA, catalogue no. 25121) was used instead of the fluorochrome-conjugated anti-mouse IgG. After a 1-hr incubation and three washes, the samples were fixed with 2% glutaraldehyde in 0.1 M cacodylate buffer (pH 7.2) containing 4% sucrose and 10 μM CaCl_2 . After osmication, the ultrasmall gold particles were silver-enhanced for 7 min at room temperature by using the Aurion-R-Gent silver enhancement kit (Electron Microscopy Sciences, Fort Washington, PA). The samples were then dehydrated and embedded in plastic for electron microscopy. Stained sections were examined with a JEOL 1200EX-II electron microscope.

Postembedding Electron Microscopy. After the short-term culture in the presence or absence of BFA, the infected erythrocytes were fixed in 0.1 M cacodylate buffer (pH 7.2) containing 0.2% glutaraldehyde, 4% sucrose, and 10 μM CaCl_2 . The osmium and uranyl treatments were omitted and the partially dehydrated samples were embedded in LR White and polymerized at 55°C. After sectioning, the sections on nickel grids were sequentially incubated with the mAbs and with anti-mouse anti-IgG coupled to 6-nm colloidal gold. Unstained grids were examined with the electron microscope at 20–40 kV and stained grids were examined at 80 kV.

RESULTS AND DISCUSSION

To study the extraparasite transport of proteins, *P. berghei*-infected erythrocytes were treated with BFA and examined by immunofluorescence microscopy using antibodies against proteins that are exported into different compartments within the host erythrocyte (Table 1). One such exported protein, Pb(em)65, is a 65-kDa protein that is localized to the eryth-

Table 1. Summary of antibodies

Antibody	Protein	Location	Species	Ref(s).
mAb 16.3	Pb(em)65	Erythrocyte membrane	<i>P. berghei</i>	19
mAb I2.6	Pb(ec)31	Cytoplasmic inclusion	<i>P. berghei</i>	17, 22
mAb W3.5	Pb(ec)13	Cytoplasmic inclusion	<i>P. berghei</i> <i>P. chabaudi</i>	17, 25
mAb F4.4	MSP-1	Parasite membrane	<i>P. berghei</i>	17, 18
mAb 13.5	Pc(em)93	Erythrocyte membrane	<i>P. chabaudi</i>	19
Anti-3008	Ag-3008	PVM, dense granules	<i>P. chabaudi</i>	20
Anti-BiP	BiP	ER	<i>P. falciparum</i> <i>P. berghei</i>	7, 21

For each of the mAbs or monospecific polyclonal rabbit antibodies used in this study, the recognized proteins, their locations, and the species are indicated. Cytoplasmic inclusion refers to a nonmembrane bound structure in the erythrocyte cytoplasm.

rocyte membrane (19). After BFA treatment Pb(em)65 is associated with the parasite in some infected erythrocytes (Fig. 1B). A similar phenomenon is also observed with Pb(ec)31 (Fig. 1D) and Pb(ec)13 (data not shown), which are normally localized to nonmembrane bound inclusions within the erythrocyte cytoplasm (17). A single BFA-induced structure of various sizes is observed per parasite. These BFA-induced structures are first observed after approximately 30 min of treatment and the maximum effect occurs after 2–4 hr of treatment. This BFA-induced structure is most prominent in erythrocytes containing less of the exported proteins (i.e., showing little or no fluorescence associated with the erythrocyte membrane or with cytoplasmic inclusions). These results suggest that BFA only blocks the export of newly synthesized proteins and leads to their accumulation in this novel compartment but does not affect proteins already exported to their final destinations.

As a control for the parasite's normal secretory pathway, the BFA-treated samples were also analyzed with a mAb raised against a parasite membrane protein known as MSP-1. Treatment with BFA blocks the transport of MSP-1 to the parasite membrane and results in the accumulation of MSP-1 in the parasite cytoplasm (Fig. 1F). The fluorescence is not an evenly disperse staining as observed for known cytosolic proteins (23) but appears mottled, suggesting that MSP-1 is now associated with vesicles. A similar immunofluorescence pattern has been reported for *P. falciparum* BiP (8), a molecular chaperon that resides in the lumen of the ER (7), and this same mottled cytoplasmic staining is also observed in *P. berghei* (Fig. 1G). Treatment with BFA does not affect the pattern of anti-BiP staining (data not shown). The similarity of the mAb F4.4 fluorescence pattern with that of an ER marker and the observation that the *Plasmodium* ER is a loose network of vesicles (5, 6) suggest that MSP-1, as expected (11), is accumulating in the ER after BFA treatment. Therefore, Pb(em)65 and Pb(ec)31 are not traversing through the ER and Golgi but are accumulating in a previously unrecognized compartment.

The effect of BFA treatment on the export of a 93-kDa erythrocyte-membrane-associated protein, Pc(em)93, was determined in a synchronous *P. chabaudi* infection (Fig. 2). Pc(em)93 is synthesized exclusively during the early ring stage (19) and then rapidly transported to the erythrocyte membrane (24). BFA treatment of *P. chabaudi*-infected erythrocytes during the early ring stage blocks the transport of Pc(em)93 to the erythrocyte membrane and leads to its accumulation in a structure similar to that observed for Pb(em)65 and Pb(ec)31. The BFA-induced structure is not observed if infected erythrocytes are treated during periods

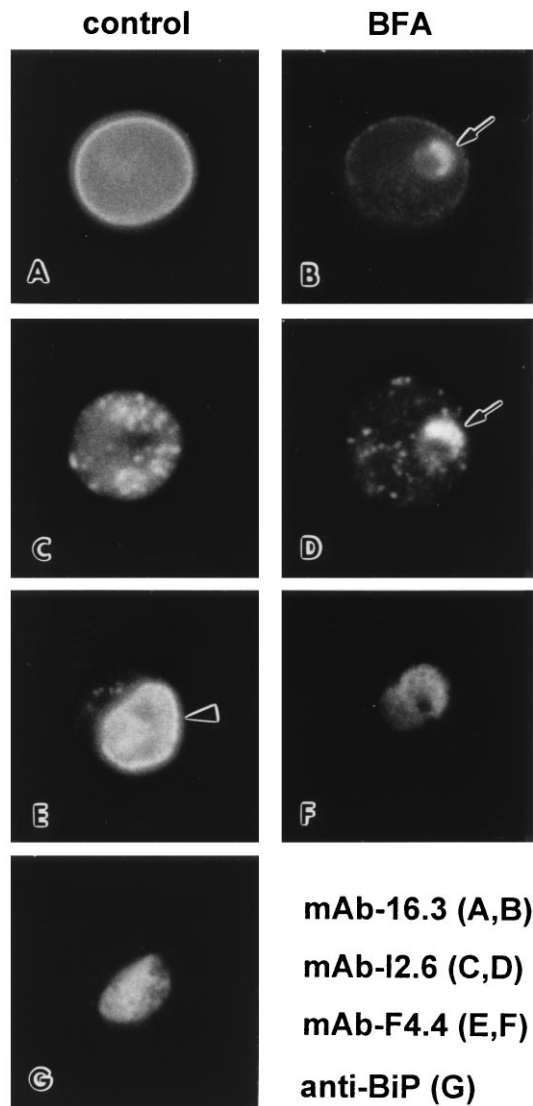


FIG. 1. Effect of BFA on the transport of *P. berghei* proteins. *P. berghei*-infected erythrocytes were incubated for 2 hr in the presence (B, D, and F) or absence (A, C, E, and G) of BFA (10 μ g/ml) and analyzed by immunofluorescence using mAb 16.3 (A and B), mAb I2.6 (C and D), mAb F4.4 (E and F), or rabbit anti-BiP (G). For the exported proteins, treatment with BFA results in the accumulation of Pb(em)65 (B) and Pb(ec)31 (D) in parasite-associated structures (arrows). MSP-1, which is normally localized to the parasite surface (emphasized with arrowhead), accumulates in the cytoplasm of the parasite after BFA treatment (D) in a pattern similar to the ER marker BiP (G).

not coinciding with the synthesis of Pc(em)93, thus confirming that BFA only inhibits the transport of newly synthesized Pc(em)93 and does not affect Pc(em)93 already associated with the erythrocyte membrane. Likewise, BFA only blocks the export of the 19-kDa *P. chabaudi* protein recognized by mAb W3.5 (25) during the late trophozoite and schizont stages coincident with its synthesis (data not shown). Counterstaining with ethidium bromide reveals a single BFA-induced structure per parasite at the periphery of the parasite (Fig. 2A). Scanning confocal fluorescence microscopy (Fig. 2B–F) indicates that there is little overlap between the ethidium bromide staining compartment (i.e., parasite RNA and DNA) and the compartment containing the accumulated Pc(em)93. In this particular parasite the BFA-induced structure is larger than normal and appears as large as the parasite itself. The lack of host membrane fluorescence and relatively small size of the parasite suggests that it is a recently invaded erythrocyte.

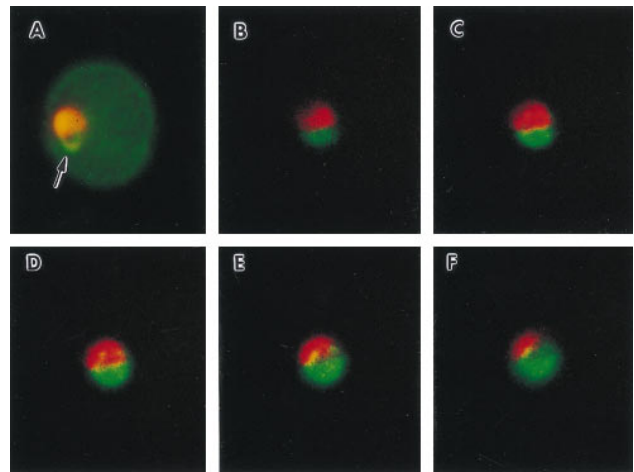


FIG. 2. Inhibition of the transport of Pc(em)93 with BFA. *P. chabaudi*-infected erythrocytes were collected during a period of maximum schizont rupture and merozoite invasion, cultured with BFA (10 μ g/ml), and analyzed by immunofluorescence using mAb 13.5 (green). Parasites were counterstained with ethidium bromide (orange or red). The samples were either analyzed by conventional immunofluorescence microscopy (A) or scanning confocal immunofluorescence microscopy (B–F). The five confocal frames are consecutive 0.5- μ m optical sections. Treatment with BFA results in the accumulation of Pc(em)93 into a compartment at the parasite periphery (arrow).

Morphologically similar BFA-induced structures have also been reported in *P. falciparum* for Ag-Pf332 and the glycoporphin-binding protein. Ag-Pf332 (14), which is associated with the cytoplasmic face of the erythrocyte membrane, and the glycoporphin-binding protein (15), which is associated with nonmembrane bound cytoplasmic inclusions, both accumulate in the parasite after BFA treatment. These investigators reported that the BFA-induced structures were in the perinuclear region of the parasite. This interpretation of the subcellular location of *P. falciparum* antigens after BFA treatment was due to a misconception that propidium iodide only stained DNA, thereby confusing the parasite-associated fluorescence for nuclear fluorescence. Propidium iodide stains both DNA and RNA (26) and malarial parasites counterstained with propidium iodide are indistinguishable from those stained with ethidium bromide (data not shown).

Dyer *et al.* (27) have also reported an immunofluorescence pattern at the parasite periphery, which is similar to that of the BFA-induced structures. These antibodies were raised against a *P. falciparum* P-type ATPase called PfATPase4. PfATPase4 and PfATPase6, another *Plasmodium* P-type ATPase, are homologous to the Ca²⁺-ATPase of the ER. The original antibody used in the PfATPase4 immunofluorescence studies (27) is no longer available, and therefore, it cannot be determined at this time whether PfATPase4 localizes to the BFA-induced compartment. Nonetheless, because of its location at the parasite periphery and homology to the ER Ca²⁺-ATPase, we propose that PfATPase4 resides in the novel BFA-induced compartment. The BFA-induced accumulation of exported *Plasmodium* proteins into a compartment distinct from the ER implies that the parasite has two ER-like organelles. The expression of two distinct organellar Ca²⁺-ATPase genes during the blood stage (27, 28) is also consistent with the malaria parasite having two ER-like organelles. One of these ER-like organelles is analogous to the ER of other eukaryotic cells, as represented by the compartment labeled with anti-BiP, and is responsible for the intracellular transport of proteins to the parasite membrane (e.g., MSP-1) and other intraparasite organelles. PfATPase6 presumably resides in this ER, but no localization data are currently available. The other ER-like

organelle is located at the parasite periphery and specializes in exporting proteins into the host erythrocyte. In anticipation of detecting similar ER-like compartments for protein export in other apicomplexa, we propose to call this other ER-like compartment the secondary ER of apicomplexa or sERA.

Presumably exported *Plasmodium* proteins will contain signal sequences that target them to the sERA. Many exported *P. falciparum* proteins contain typical signal sequences (29, 30), and a few of these proteins translocate across microsomal membranes *in vitro* (30). Comparison of N-terminal amino acids[†] from Pc(em)93 with other *P. chabaudi* proteins, including the parasite-membrane-associated MSP-1, the rhoptry-associated AMA-1, the dense-granule-associated Ag-3008, and the erythrocyte-membrane-associated PcEMP-1 revealed typical signal sequences (31) in all five proteins (data not shown), and no distinctions between proteins exported into the erythrocyte and proteins associated with intraparasite compartments were noted. In light of the observation that BFA prevents the cleavage of the signal sequence from rhoptry proteins (32, 33), the sizes of Pc(em)93, Pb(em)65, and Pb(ec)31 from BFA-treated and control cells were compared, and no size differences were detected (R.A.B. and M.F.W., unpublished results). Determining the nature of the potential sERA signal sequences will probably require an empirical approach involving the parasite transfection (34).

Ag-3008 is a 24-kDa *P. chabaudi* protein that has been previously localized to the PVM and to cytoplasmic clefts within trophozoite-infected erythrocytes (20). During the schizont and merozoite stages, this protein is associated with the dense granules. Presumably Ag-3008 is synthesized during the schizont stage and then transferred to the PVM as a result of dense granule release occurring after merozoite invasion (35). BFA treatment of infected erythrocytes during the early ring stage, but not at other times in the schizogonic cycle, results in the accumulation of Ag-3008 in the BFA-induced structure (Fig. 3). This suggests that BFA treatment can affect the secretion of both newly synthesized proteins and proteins synthesized in the previous replicative cycle but still in transit to their final destination at the time of BFA treatment. Furthermore, both Ag-3008 and Pc(em)93 are localized to the same BFA-induced compartment (Fig. 3), indicating that the parasite has a single sERA. The BFA block of Pc(em)93 and Ag-3008 export also indicates that the sERA is established immediately after merozoite invasion. Interestingly, PfAT-Pase4 is also expressed maximally during the ring stage (27). After its establishment, the sERA then remains in operation throughout the schizogonic cycle since proteins that are exported in the trophozoite and schizont stages also utilize this pathway.

The observation that Ag-3008 uses the sERA also implies that dense granules may participate in the establishment of this alternate secretory pathway. Dense granules are analogous to secretory vesicles and are well characterized in *Toxoplasma* (36). In *Toxoplasma* tachyzoites, the exocytosis of dense granules occurs at the apical end within minutes after invasion, suggesting that there are predetermined sites for exocytosis (37). Just prior to exocytosis, membranous formations are observed in many of the dense granules (38). Interestingly, *Toxoplasma* dense granule proteins are differentially targeted to the PVM and to an intravacuolar network of membranes found within the parasitophorous vacuole (36). Similarly, *Plasmodium* dense granule proteins are differentially sorted to the erythrocyte membrane (39, 40), to the PVM (20), and to the parasite membrane (41). The differential targeting of these dense granule proteins could provide a framework for the alternate secretory pathway that then functions throughout the

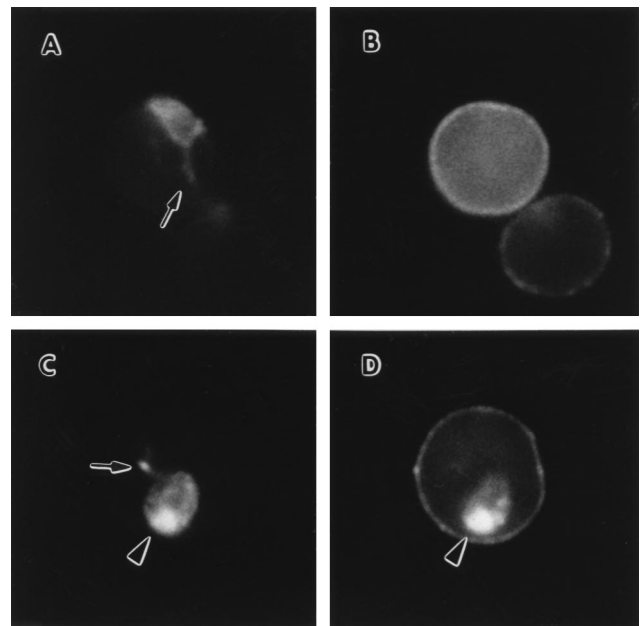


FIG. 3. Dual labeling experiments using antibodies against Pc(em)93 and a PVM-associated protein. *P. chabaudi*-infected erythrocytes were analyzed by immunofluorescence in controls (A and B) and after BFA treatment (C and D) with a mixture of mAb 13.5 and rabbit anti-Ag-3008. The second antibodies were rhodamine-conjugated anti-mouse IgG and fluorescein-conjugated anti-rabbit IgG. Examination of the same fields for epifluorescence using filters exclusive for either fluorescein (A and C) or rhodamine (B and D) revealed a green fluorescence associated with the PVM (A) and a red fluorescence associated with the erythrocyte membrane (B) in the control. The BFA-induced structure (arrowheads) fluoresces both green (C) and red (D), indicating a colocalization of Pc(em)93 and Ag-3008. Arrows denote membranous PVM extensions corresponding to cytoplasmic clefts. Examination of samples only treated with one of the primary antibodies revealed little cross-over of the fluorochromes between the filter combinations (data not shown).

remainder of the schizogonic cycle. Similarly, the establishment of the alternate secretory pathway in the early ring stage immediately after invasion suggests that other apical organelles could also play a role in the formation of the sERA. For example, at the time of invasion the contents of the rhoptries and micronemes are released and specialized domains on the parasite plasma membrane may be formed as a result. Alternatively, specialized membrane domains may already be present in the merozoite and these domains would serve as a foundation for the establishment of the sERA.

Initial attempts to characterize the BFA-induced structure at the ultrastructural level by using conventional immunoelectron microscopy techniques were not successful. Therefore, the immunofluorescence procedure was modified by using an ultrasmall gold-conjugated second antibody that behaves similar to fluorochrome-conjugated second antibodies (42). The ultrasmall gold is subsequently detected after silver enhancement. Examination of the BFA-treated *P. chabaudi*-infected erythrocytes by using the preembedding immunogold labeling followed by silver enhancement shows that label is associated with the erythrocyte membrane and with the parasite (Fig. 4A). Gold particles are not dispersed throughout the cytoplasm of the BFA-treated parasite but are found in clusters near the parasite periphery. A similar distribution of gold particles is also observed in *P. berghei*-infected erythrocytes treated with BFA and labeled with mAb 16.3 (data not shown). The gold particles appear to identify a membrane bound compartment that is distinct from the parasite cytoplasm (Fig. 4A, arrowheads). The required detergent permeabilization step (22) and the low concentration of glu-

[†]The GenBank accession numbers for the five sequences are U80896, M34947, M25248, L19784, and M95789.

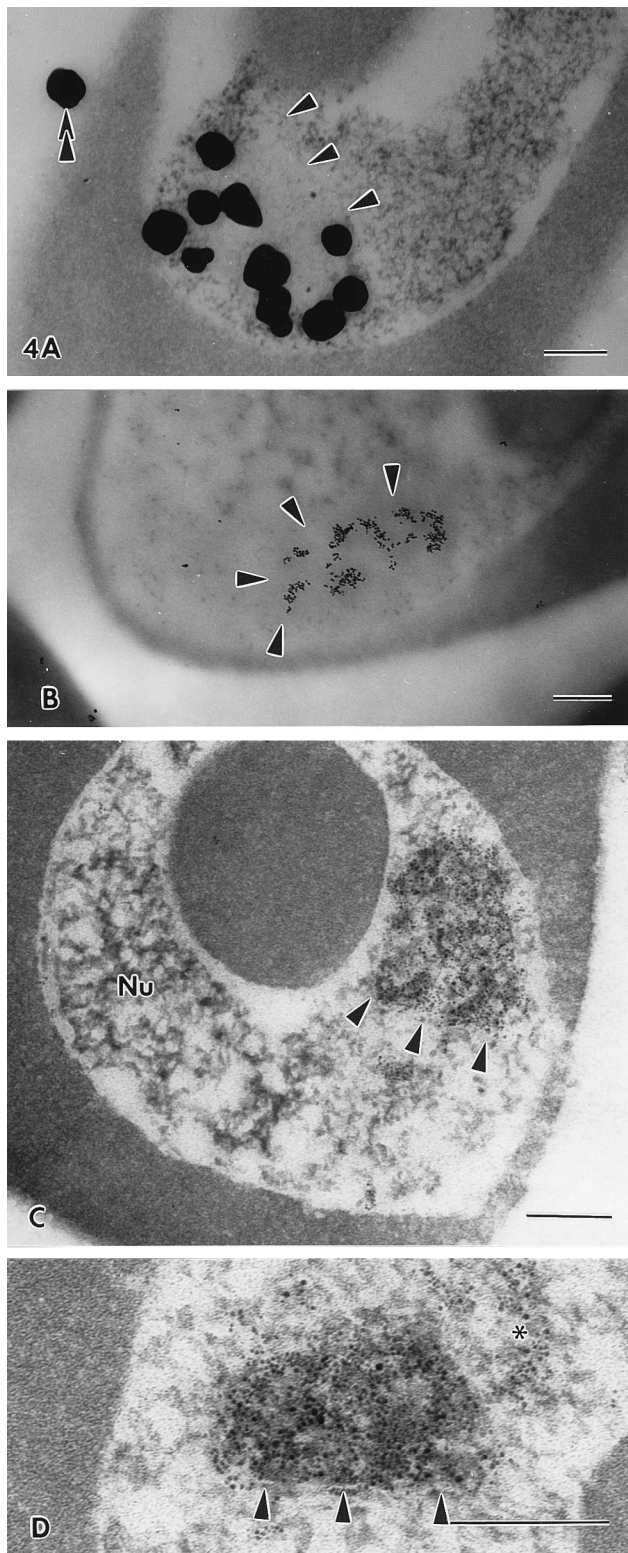


FIG. 4. Immunogold localization of Pc(em)93 after BFA treatment. Arrowheads denote a boundary between the BFA-induced compartment and the parasite cytoplasm (Bars = 200 nm.) (A) *P. chabaudi*-infected erythrocytes were treated with BFA as described in Fig. 2 and processed for preembedding immunogold electron microscopy. A single cluster of silver-enhanced gold particles is found within the parasite near its periphery. The double arrowhead points to a silver grain on the erythrocyte membrane. (B) *P. chabaudi*-infected erythrocytes were treated with BFA and examined by postembedding localization with mAb 13.5. Examination of unstained grids under low voltage reveals a colocalization of gold particles with a distinct intraparasitic compartment. (C and D) Gold particles colocalize with

taraldehyde used for the primary fixation adversely affects the ultrastructure and precludes the ability to detect a distinct membrane. The BFA-induced compartment was not detected if the infected erythrocytes were permeabilized with saponin instead of Triton X-100 (data not shown). This is further evidence that the sERA is inside the parasite since saponin only permeabilizes the erythrocyte membrane and the PVM and not the parasite plasma membrane (43).

P. chabaudi-infected erythrocytes were fixed with 0.2% glutaraldehyde and examined by postembedding labeling using mAb 13.5. As with preembedding labeling, clusters of gold particles were observed in BFA-treated parasites (Fig. 4 B–D). The gold particles are associated with structures that stain relatively intensely after on-grid contrasting with uranyl acetate and lead citrate (Fig. 4 C and D). The reason for the intense staining is not clear at this time but is possibly due to the high negative charge of Pc(em)93 (19). Equivalent grids were not stained and examined under low voltage. Again the gold label is associated with an intraparasite compartment that appears distinct from the rest of the parasite's cytoplasm (Fig. 4B). The low concentration of glutaraldehyde used for fixation probably precludes the ability to detect membranes. Alternatively, the sERA may be a nonmembrane bound compartment involved in the export of proteins from the parasite. However, preliminary density gradient centrifugation analysis demonstrate that the BFA-induced compartment is recovered in fractions containing membranes (M.F.W. and D. J. Grab, unpublished results).

Infected erythrocytes treated with BFA were also examined by conventional transmission electron microscopy. No major morphological differences between the controls and the treated erythrocytes were observed. Crary and Haldar (12) also did not observe any major morphological changes in *P. falciparum* after BFA treatment. This inability to detect this novel BFA-induced structure suggests either that the ultrastructural attributes of the sERA are subtle or that they are not preserved during routine fixation and embedding procedures. In summary, we propose that the sERA is a membrane bound compartment located near the periphery of the parasite and exhibits many ER-like properties. However, the sERA is clearly distinct from the ER as demonstrated by immunofluorescence (Fig. 1). Furthermore, comparison of previously published immunogold labeling using anti-BiP antibodies (7) with those of exported proteins following BFA treatment (Fig. 4) confirms that the EA and the sERA are distinct compartments.

Exported proteins destined for different intraerythrocytic locations accumulate in the sERA after BFA treatment, indicating that sorting occurs after this compartment. A tubovesicular membrane (TVM) network extending from the PVM throughout the erythrocyte cytoplasm has been described (44). Interestingly, sphingomyelin synthetase, a Golgi marker, is associated with this TVM network, suggesting that the PVM and associated membranous extensions exhibit similarities to the Golgi. Therefore, by analogy, exported proteins may proceed from the sERA to the TVM network where sorting takes place. However, the sERA and PVM are separated by the parasite plasma membrane, suggesting an intermediate compartment. In this regard, the glycophorin-binding protein traverses the parasitophorous vacuole in route to the erythrocyte cytoplasm (45), suggesting that exported proteins move from the sERA to the parasitophorous vacuole before becoming associated with the PVM or TVM network. BFA blocks secretion by inhibiting the formation of transfer vesicles

an intraparasitic structures that stains intensely with uranyl acetate and lead citrate. This structure is not associated with the nucleus (Nu). The asterisk marks gold particles outside the BFA-induced compartment, possibly due to leakage resulting from the low glutaraldehyde fixation.

that move proteins from the ER to the Golgi (11). More specifically BFA inhibits the guanine nucleotide exchange on a Ras-like G protein (46). Similar Ras-like G proteins have been recently identified in *P. falciparum* (9, 10). The BFA inhibition implies that proteins move from the sERA to the parasitophorous vacuole via transfer vesicles. Alternatively, the juxtaposition of the sERA with the parasite plasma membrane suggests that exported proteins could move into the parasitophorous vacuole via more direct connections but still involving G proteins.

In summary, malarial parasites, and probably other apicomplexa, have two secretory pathways. One is analogous to the normal secretory pathway that targets proteins to the parasite membrane and other intraparasite organelles. The other secretory pathway specializes in targeting proteins to compartments within the host cell. An early step in the export process involves an ER-like compartment called the sERA. This model of export differs slightly from other proposed models in which the classical ER and Golgi are involved in the export of *Plasmodium* proteins (47). The origin of sERA, the targeting of proteins to sERA, and the fate of proteins after traversing sERA remain to be determined.

We thank Ms. Maryetta Brooks for superb technical assistance, Dr. Dennis Grab for his continuous consults and for critically reading this manuscript, and Dr. Nirbhay Kumar (John Hopkins University) for supplying the anti-BiP. This work was funded by National Institutes of Health Grant AI31083 and H.N.L. was also supported in part by National Institutes of Health Grant PR00164-32.

1. Aikawa, M. (1977) *Bull. W.H.O.* **55**, 139–156.
2. Stenzel, D. J. & Kara, U. A. K. (1989) *Eur. J. Cell Biol.* **49**, 311–318.
3. Gormley, J. A., Howard, R. J. & Taraschi, T. F. (1992) *J. Cell Biol.* **119**, 1481–1495.
4. Rothman, J. E. (1994) *Nature (London)* **372**, 55–63.
5. Aikawa, M. (1971) *Exp. Parasitol.* **30**, 284–320.
6. Langreth, S. G., Jensen, J. B., Reese, R. T. & Trager, W. (1978) *J. Protozool.* **25**, 443–452.
7. Kumar, N., Koski, G., Harada, M., Aikawa, M. & Hong, Z. (1991) *Mol. Biochem. Parasitol.* **48**, 47–58.
8. Elmendorf, H. G. & Haldar, K. (1993) *EMBO J.* **12**, 4763–4773.
9. Stafford, W. H. L., Stockley, R. W., Ludbrook, S. B. & Holder, A. A. (1996) *Eur. J. Biochem.* **242**, 104–113.
10. Ward, G. E., Tilney, L. G. & Langsley, G. (1997) *Parasitol. Today* **13**, 57–62.
11. Klausner, R. D., Donaldson, J. G. & Lippincott-Schwartz, J. (1992) *J. Cell Biol.* **116**, 1071–1080.
12. Crary, J. L. & Haldar, K. (1992) *Mol. Biochem. Parasitol.* **53**, 185–192.
13. Elmendorf, H. G., Bangs, J. D. & Haldar, K. (1992) *Mol. Biochem. Parasitol.* **52**, 215–230.
14. Hinterberg, K., Scherf, A., Gysin, J., Toyoshima, T., Aikawa, M., Mazie, J. C., Pereira da Silva, L. & Mattei, D. (1994) *Exp. Parasitol.* **79**, 279–291.
15. Benting, J., Mattei, D. & Lingelbach, K. (1994) *Biochem. J.* **300**, 821–826.
16. Trager, W. & Jensen, J. B. (1976) *Science* **193**, 673–675.
17. Wiser, M. F. (1986) *Eur. J. Cell Biol.* **42**, 45–51.
18. Toebe, C. S., Clements, J. D., Cardenas, L., Jennings, G. J. & Wiser, M. F. (1997) *Am. J. Trop. Med. Hyg.* **56**, 192–199.
19. Wiser, M. F., Leible, M. B. & Plitt, B. (1988) *Mol. Biochem. Parasitol.* **27**, 11–22.
20. Favaloro, J. M., Culvenor, J. G., Anders, R. F. & Kemp, D. J. (1993) *Mol. Biochem. Parasitol.* **62**, 263–270.
21. Kumar, N., Nagasawa, H., Sacci, J. B., Jr., Sina, B. J., Aikawa, M., Atkinson, C., Uparanukraw, P., Kubiak, L. B., Azad, A. F. & Hollingdale, M. R. (1993) *Parasitol. Res.* **79**, 109–113.
22. Wiser, M. F., Faur, L. V. V., Lanners, H. N., Kelly, M. & Wilson, R. B. (1993) *Parasitol. Res.* **79**, 579–588.
23. Wiser, M. F., Jennings, G. J., Uparanukraw, P., van Belkum, A., van Doorn, L. J. & Kumar, N. (1996) *Mol. Biochem. Parasitol.* **83**, 25–33.
24. Wiser, M. F. & Lanners, H. N. (1992) *Parasitol. Res.* **78**, 193–200.
25. Wiser, M. F. (1989) *Parasitol. Res.* **75**, 206–211.
26. Kawamoto, F. & Kumada, N. (1987) *Parasitol. Today* **3**, 284–286.
27. Dyer, M., Jackson, M., McWhinney, C., Zhao, G. & Mikkelsen, R. (1996) *Mol. Biochem. Parasitol.* **78**, 1–12.
28. Kimura, M., Yamaguchi, Y., Takada, S. & Tanabe, K. (1993) *J. Cell Sci.* **104**, 1129–1136.
29. Braun-Breton, C., Langsley, G., Mattei, D. & Scherf, A. (1990) *Blood Cells* **16**, 396–400.
30. Lingelbach, K. R. (1993) *Exp. Parasitol.* **76**, 318–327.
31. von Heijne, G. (1985) *J. Mol. Biol.* **184**, 99–105.
32. Ogun, S. A. & Holder, A. A. (1994) *Exp. Parasitol.* **79**, 270–278.
33. Howard, R. F. & Schmidt, C. M. (1995) *Mol. Biochem. Parasitol.* **74**, 43–54.
34. van Dijk, M. R., Waters, A. P. & Janse, C. J. (1995) *Science* **268**, 1358–1362.
35. Bannister, L. H., Butcher, G. A., Dennis, E. D. & Mitchell, G. H. (1971) *Parasitology* **71**, 483–491.
36. Cesbron-Delauw, M. F. (1994) *Parasitol. Today* **10**, 293–296.
37. Dubremetz, J. F., Achbarou, A., Bermudes, D. & Joiner, K. A. (1994) *Parasitol. Res.* **79**, 402–408.
38. Charif, H., Darcy, F., Torpier, G., Cesbron-Delauw, M. F. & Capron, A. (1990) *Exp. Parasitol.* **71**, 114–124.
39. Aikawa, M., Torii, M., Sjolander, A., Berzins, K., Perlman, P. & Miller, L. H. (1990) *Exp. Parasitol.* **71**, 326–329.
40. Culvenor, J. G. & Anders, R. F. (1991) *Infect. Immun.* **59**, 1183–1187.
41. Trager, W., Rozario, C., Shio, H., Williams, J. & Perkins, M. E. (1992) *Infect. Immun.* **60**, 4056–4661.
42. Hainfeld, J. F. (1988) *Nature (London)* **333**, 281–282.
43. Izumo, A., Tanabe, K. & Kato, M. (1987) *Trans. R. Soc. Trop. Med. Hyg.* **81**, 264–267.
44. Elmendorf, H. G. & Haldar, K. (1994) *J. Cell Biol.* **124**, 449–462.
45. Anson, I., Benting, J., Bhakdi, S. & Lingelbach, K. (1996) *Biochem. J.* **315**, 307–314.
46. Donaldson, J. G. & Klausner, R. D. (1994) *Curr. Opin. Cell Biol.* **6**, 527–532.
47. Haldar, K. (1996) *Trends Cell Biol.* **6**, 398–405.